2026 IEEE Transportation Electrification Conference & Expo (ITEC) & Electric Aircraft Technologies Symposium (EATS) (ITEC+EATS) | 979-8-3315-8773-4/26/$31.00 ©2026 IEEE | DOI: 10.1109/ITECEATS66641.2026.11593039

Robust Data-Enabled Predictive Control for EV Charging under Thermal Constraints

Luke Nuculaj
ECE, Oakland University
Rochester, MI, USA
lukenuculaj@oakland.edu

Wanqun Yang
ECE, Oakland University
Rochester, MI, USA
wanqunyang@oakland.edu

Jun Chen*
ECE, Oakland University
Rochester, MI, USA
junchen@oakland.edu

***Abstract*—This work builds upon predictive control strategies for optimal charging of lithium batteries under thermal constraints by extending the problem to data-enabled predictive control (DeePC), which uses data-driven Hankel matrices generated offline for real-time prediction in lieu of an explicit model. Moreover, the robust framework for DeePC is considered for the case of noisy Hankel matrix data, and the nonlinear robustness constraint is tightened to a linear constraint, ensuring compatibility with standard quadratic programming (QP) solvers. Simulation results demonstrate that the proposed DeePC framework successfully navigates the trade-off between fast charging and thermal safety, achieving convergence within 1% of the reference SOC after 500 seconds under specific tuning while maintaining core temperatures in a safe vicinity. Under conservative tunings, the controller exhibits a charging rate of 0.816C, remaining within the recommended safe range to mitigate early-life plating. Hence, the DeePC approach as a viable control framework for generating charging strategies is validated.**

***Index Terms*—Electric vehicles, optimal charging, lithium-ion batteries, data-enabled predictive control, thermal runaway**

I. Introduction

In recent times, environmentally-friendly technologies such as electric vehicles (EVs) and smart grids have become all but ubiquitous as the global community strives to reduce carbon emissions [1], [2]. Lithium-ion batteries lie at the core of these technologies due to their high energy density, long lifetimes, fast charging capability, and affordability [3]. However, the rapid growth of battery-powered applications has heightened the risk of unsafe charging practices, with several reported involving fire damage, thermal runaway, and even personal injury resulting from overcharging [4]. To address these concerns, extensive research has focused on developing safe and accurate charging strategy, which generally fall into two categories. First, model-free charging techniques such as constant-current–constant-voltage (CC–CV), multistage constant current (MSCC), and pulse charging are revered for their tradeoff between simplicity and efficacy [5], [6]. While they do not require mathematical battery models and can reduce control development time, there is a lack of optimality guarantee in these model-free methods. On the other hand, model-based charging strategies rely on mathematical battery models to estimate internal states and parameters of interest, which can, in turn, contribute to the efficiency and overall safety of charging strategies relative to model-free methods [7]. However, many of the model-based methods in question are subject to a tradeoff between model accuracy and computational efficiency. In this context, much literature has pointed towards the equivalent circuit model (ECM) as a sufficient modeling tool that strikes a balance between accuracy and computational complexity [8]. Still, such a model requires accurate knowledge of the equivalent circuit parameters, which are generally difficult to ascertain exactly and instead must be estimated.

In the scope of model-based charging methods, model predictive control (MPC) has positioned itself as the dominant control optimization strategy for its ability to generate optimal charging strategies that optimize some prespecified performance criterion while also abiding by both system and design constraints [9], [10]. For reasons mentioned earlier, the ability to predict—and consequently, the performance—of the MPC controller can be hindered if the model is not a sufficiently accurate approximation of system behavior [11]. To this end, recent pushes in the optimal control literature have explored the use of data-driven techniques to predict future trajectories directly [12]–[14]. Among those available, techniques involving the use of Hankel matrices have shown great promise. Specifically, this concept stems from Willems' fundamental lemma in behavioral systems theory, which, under certain conditions and assumptions, provides a means by which future trajectories can be predicted using linear combinations derived from a set of system trajectories obtained *a priori* [11], [12]. Said system trajectories are stored in the aforementioned Hankel matrices. Such a technique, termed "data-enabled predictive control" (DeePC), offers a useful solution to the optimal charging strategy problem, bridging the gap between model-free and model-based methods [13], [14]. Namely, the system can reap the benefits provided by the foresight and optimality of a predictive controller while ensuring that minimal effort is wasted in obtaining an explicit mathematical model.

To this end, we propose the following contributions:

1) A formulation of the optimal control problem (OCP) with a quadratic objective function balancing charging speed, temperature increase, and Ohmic heat loss. The constraints are linear, incorporating the Hankel matrices

This work is supported in part by National Science Foundation through Awards #2237317 and #2430374. *Corresponding author: J. Chen.*

collected *a priori* for model prediction. The OCP will be equipped for robustness against noisy trajectories stored inside of the Hankel matrices.
2) A known constraint for robustness of DeePC is tightened to preserve linearity of constraints for an easily solvable convex quadratic programming (QP) problem.
3) Simulation-in-the-loop results are obtained reporting safe and reliable optimal control strategies while respecting thermal constraints in spite of noisy Hankel matrix data. Specifically, select parameterizations of the optimal cost show convergence to the desired SOC reference in as few as 500 seconds while keeping core battery temperature below a prescribed safety limit. Moreover, a charging rate of 0.816C is produced for more conservative weight parameterizations which more strongly penalize temperature rise and tolerate slow charging.

The rest of the paper is organized as follows. Section II outlines the mathematical notations which are adopted throughout. Section III introduces preliminary background material pertinent to DeePC (Section III-A) and formulates the robust optimal control problem for the DeePC charging strategy (Section III-B). Section IV provides a set of constraints that, when satisfied, are sufficient in satisfying the original robustness constraints while maintaining QP-solver compatibility. Section V details the target battery system along with relevant details regarding initialization, dimension, and constraints, displaying the results of fast-charging under various weights and thermal constraints. Section VI summarizes the main points of this work followed by a brief discussion for future work.

II. Notation

Let $\mathbb{R}$, $\mathbb{R}^n$, $\mathbb{R}^{m\times n}$, $\mathbb{Z}$, and $\mathbb{N}$ respectively denote the field of real numbers, the set of real column vectors of length n, the set of m-by-n real matrices, the set of integers, and the set of natural numbers. The transpose of a matrix $A \in \mathbb{R}^{m\times n}$ is denoted by $A^\top$. The ℓ_1 norm $\|x\|_1 := \sum_{i=1}^n |x_i|$, the ℓ_2 "Euclidean" norm $\|x\|_2 := \sqrt{\sum_{i=1}^n x_i^2}$, and the ℓ_∞ "infinity" norm $\|x\|_\infty := \max_i |x_i|$ for vectors. For matrices, the induced spectral norm is defined $\|A\| := \sup_{\|x\|=1} \|Ax\|$. Given a square matrix $A \in \mathbb{R}^{n\times n}$, we have the following: the weighted vector norm $\|x\|_A^2 := x^\top A x$.

For time step $k \in \mathbb{Z}_{\geq 0}$, horizon $p \in \mathbb{Z}_{>0}$, trajectory length $L \in \mathbb{Z}_{>0}$, and data point $z \in \mathbb{R}^{n_z}$, the trajectory $z_{[k,k+L]} := [z_k^\top,\ z_{k+1}^\top,\ \cdots z_{k+L}^\top]^\top \in \mathbb{R}^{n_z(L+1)}$, and $z_{[k,k+L]}$ induces the Hankel matrix

$$Z_{k,p,L-p+1} := \begin{bmatrix} z_k & z_{k+1} & \cdots & z_{k+L-p} \\ z_{k+1} & z_{k+2} & \cdots & z_{k+L-p+1} \\ \vdots & \vdots & \ddots & \vdots \\ z_{k+p-1} & z_{k+p} & \cdots & z_{k+L-1} \end{bmatrix},$$

where $Z_{k,p,L-p+1} \in \mathbb{R}^{n_z p\times(L-p+1)}$.

III. Problem Formulation

A. Background

At the basis of the data-driven control problem, we wish to control the following unknown, discrete-time system of order $n \in \mathbb{N}$:

$$x_{k+1} = f(x_k, u_k) \tag{1a}$$

$$\tilde{y}_k = h(x_k, u_k) + \varepsilon_k, \tag{1b}$$

where $u_k \in \mathbb{R}^{n_u}$ is the control input, $\tilde{y}_k \in \mathbb{R}^{n_y}$ is the measured output perturbed by added noise $\varepsilon_k \in \mathbb{R}^{n_y}$, and subscript k indicates the value of the variable as it exists at the kth discrete time step. Specifically, our goal is to generate practical control strategies using only input-output (IO) data measured ahead of time. Note that the distribution of ε_k is not required to be known, but we do impose the mild assumption that the added noise is bounded via $\|\varepsilon_k\|_\infty \leq \bar{\varepsilon}$ for some constant $\bar{\varepsilon} > 0$ known in advance; an assumption consistent with existing robust DeePC literature [14]. For the case of the optimal charging strategy, let $u_k := i_k$ and $y_k := [s_k,\ V_{p,k},\ T_{c,k}]^\top$, where $i_k \in \mathbb{R}$ is the current applied to the battery, $s_k \in \mathbb{R}_{[0,1]}$ is the SOC, $V_{p,k}$ is the relaxation voltage in Volts, and $T_{c,k}$ is the core temperature of the battery in °C. To achieve control of (1), we require a data-based prediction model. To this end, we define an input-sequence $\{u_k^d\}_{k=0}^{N-1}$ – where $N \in \mathbb{N}$ is the trajectory length – and subject the system to said input sequence. From here, the noisy outputs $\{\tilde{y}_k^d\}_{k=0}^{N-1}$ that are produced in response to the input sequence are collected; both sequences are stored in input $U_{0,p,N-p+1}$ and output $\tilde{Y}_{0,p,N-p+1}$ Hankel matrices, where $p \in \mathbb{N}$ is the prediction horizon. In order to use these Hankel matrices for model prediction, we recall the following materials, which are standard in behavioral systems theory.

Definition 1 (Reproduced from [12]). *Given control input $u_k^d \in \mathbb{R}^{n_u}$ and prediction horizon $p \in \mathbb{N}$, the input trajectory $\{u_k^d\}_{k=0}^{N-1}$ of length $N \in \mathbb{N}$ is said to be persistently exciting of order p if and only if* $\operatorname{rank}(U_{0,p,N-p+1}) = n_u p$.

However, the input trajectory $\{u_k^d\}_{k=0}^{N-1}$ must meet the "persistence of excitation" criterion as put forth in behavioral systems theory, which is satisfied if $\operatorname{rank}(U_{0,p,N-p+1}) = n_u p$, where $p \in \mathbb{N}$ is the prediction horizon. For more details regarding how to design persistently-exciting control trajectories, we refer the reader to Section V. From here, persistent excitation lends itself to a known theorem regarding linear time-invariant (LTI) systems, which we restate as follows.

Theorem 1 (Reproduced from [11]). *Suppose (1) is an LTI system of order $n \in \mathbb{N}$, producing the IO trajectory $\{u_k^d, \tilde{y}_k^d\}_{k=0}^{N-1}$, where $\{u_k^d\}_{k=0}^{N-1}$ is persistently exciting of order $n + p$. Moreover, let $U_{0,n+p,N-n-p+1}$ and $\tilde{Y}_{0,n+p,N-n-p+1}$ be the Hankel matrices induced by the IO trajectory. Then, $\{\bar{u}_k, \bar{y}_k\}_{k=i}^{i+n+p-1}$ is a trajectory of the LTI system if and only if there exists $\alpha \in \mathbb{R}^{N-n-p+1}$ such that*

$$\begin{bmatrix} \bar{u} \\ \bar{y} \end{bmatrix} = \begin{bmatrix} U_{0,n+p,N-n-p+1} \\ \tilde{Y}_{0,n+p,N-n-p+1} \end{bmatrix} \alpha.$$

In essence, Theorem 1 states that any realizable IO trajectory of the system can be constructed by an appropriate linear combination (i.e., α) of the columns of the augmented Hankel matrix. The condition is both necessary and sufficient: if no such α exists, the system cannot generate the trajectory, and vice versa. This insight is especially valuable when an explicit system model is difficult to obtain. For further background on behavioral systems theory and Willems' fundamental lemma, we refer the reader to [12]–[15]. From here, two challenges emerge. *First*, no assumptions of linearity or time-invariance can be made on the unknown system (1), so Theorem 1 may not hold under nonlinear dynamics, as is common in lithium battery systems. *Second*, noise in $\{\tilde{y}_k^d\}_{k=0}^{N-1}$ can distort the row span of the augmented Hankel matrix, degrading prediction accuracy.

B. Robust Optimal Control Problem

Towards an optimal control strategy, consider the case where the Hankel matrices may contain noise due to imprecise measurement tools, as captured by ϵ_k in (1b). To address this, we utilize the following robust DeePC problem formulation as outlined in [14]:

$$\min_{\bar{u},\bar{y},\alpha,\sigma} \quad \sum_{k=0}^{p-1} \ell(\bar{u}_k, \bar{y}_k, \bar{y}_{k-1}) + \lambda_\alpha \bar{\varepsilon}\|\alpha\|_2^2 + \lambda_\sigma \|\sigma\|_2^2 \tag{2a}$$

$$\text{s.t.} \quad \begin{bmatrix} H_{n+p}(u^d) \\ H_{n+p}(\tilde{y}^d) \end{bmatrix} \alpha = \begin{bmatrix} \bar{u} \\ \bar{y} + \sigma \end{bmatrix}, \tag{2b}$$

$$\begin{bmatrix} \bar{u}_{[-n,-1]} \\ \bar{y}_{[-n,-1]} \end{bmatrix} = \begin{bmatrix} u_{[t-n,t-1]} \\ \tilde{y}_{[t-n,t-1]} \end{bmatrix}, \tag{2c}$$

$$\|\sigma_k\|_\infty \leq \bar{\varepsilon}(1 + \|\alpha\|_1), \tag{2d}$$

$$\bar{u}_k \in \mathbb{U}, \bar{y}_k \in \mathbb{Y}, \ \forall k \in \mathbb{Z}_{[0,p-1]}, \tag{2e}$$

where stage cost $\ell(\bar{u}_k, \bar{y}_k, \bar{y}_{k-1}) : \mathbb{R}^{n_u \times n_y \times n_y} \mapsto \mathbb{R}$ is defined as $\ell(\bar{u}_k, \bar{y}_k, \bar{y}_{k-1}) := \|\bar{u}_k\|_{Q_u}^2 + \|\bar{y}_k - \bar{y}_{\text{ref}}\|_{Q_y}^2 + \|M_t(\bar{y}_k - \bar{y}_{k-1})\|_{Q_{\text{tr}}}^2$ for $k \in \mathbb{Z}_{\geq 0}$, where we note y_{-1} is the measurement from the previous time step. Moreover, matrices $Q_u := q_i \in \mathbb{R}$, $Q_y := \text{diag}\{q_s,\ q_V,\ 0\} \in \mathbb{R}^{3\times 3}$, $Q_{\text{tr}} = \text{diag}\{0,\ 0,\ q_{\text{tr}}\} \in \mathbb{R}^{3\times 3}$, $M_t := \begin{bmatrix} 0 & 0 & 1 \end{bmatrix}$, with penalties on Ohmic heat loss ($q_i, q_V \in \mathbb{R}_{\geq 0}$), distance from reference SOC ($q_s \in \mathbb{R}_{\geq 0}$), and temperature rise ($q_{\text{tr}} \in \mathbb{R}_{\geq 0}$). Constraint (2c) enforces the result from Theorem 1 with the addition of a compensatory slack variable $\sigma \in \mathbb{R}^{n_y(n+p)}$, and an equality constraint on the initial condition, ensuring that the optimal IO sequence agrees with the past n data points. Constraint (2d) ensures that the optimal trajectory lies in constraint sets $\mathbb{U}$ and $\mathbb{Y}$, and that the magnitude of σ is bounded above by the noise bound $\bar{\varepsilon}$ and α, preventing the over-compensation of σ. For our constraint sets, we define $\mathbb{U} := \{i \in \mathbb{R} : i \in \mathbb{R}_{[i_{\min}, i_{\max}]}\}$ and $\mathbb{Y} := \{(s, V_p, T_c) \in \mathbb{R}^{n_y} : s \in \mathbb{R}_{[s_{\min}, s_{\max}]}, V_p \in \mathbb{R}_{[V_{p,\min}, V_{p,\max}]}, T_c \in \mathbb{R}_{[T_{c,\min}, T_{c,\max}]}\}$. As we discuss in Section IV, this constraint requires modification into a linear form.

IV. Constraint Modification

We have the constraint on robustness (2d), which is inherently nonlinear by the inclusion of the ℓ_1 norm $\|\alpha\|_1$. This reverts (2) to a non-standard QP problem, which limits its compatibility with standard QP solvers. However, we offer the following theoretical results towards a sufficient variant of (2d) that preserves linearity:

Theorem 2. *Let $\alpha \in \mathbb{R}^{N-p+1}$ and $\sigma \in \mathbb{R}^{n_y(n+p)}$ be vectors which satisfy*

$$-D\sigma + \bar{\epsilon}\alpha \leq t, \quad D\sigma - \bar{\epsilon}\alpha \leq t,$$

where $D := [I_{n+p} \mid 0_{(n+p)\times(N-2n-2p+1)}]^\top \in \mathbb{R}^{(N-n-p+1)\times(n+p)}$, $t := [\bar{\varepsilon} \ \ \bar{\varepsilon} \ \ \dots \ \ \bar{\varepsilon}]^\top \in \mathbb{R}^{N-n-p+1}$, and $\epsilon_k \leq \bar{\epsilon} \in \mathbb{R}_{>0}$ for all $k \in \mathbb{Z}_{\geq 0}$. Then, $\|\sigma_k\|_\infty \leq \bar{\epsilon}(1 + \|\alpha\|_1)$ is necessarily satisfied.

Proof. Starting with $-D\sigma + \bar{\epsilon}\alpha \leq t$ and $D\sigma - \bar{\epsilon}\alpha \leq t$, we have the following:

$$\begin{aligned}
&-D\sigma + \bar{\epsilon}\alpha \leq t,\ D\sigma - \bar{\epsilon}\alpha \leq t \\
&\iff \|D\sigma - \bar{\epsilon}\alpha\|_\infty \leq \bar{\epsilon}, \\
&\implies \|D\sigma\|_\infty - \bar{\epsilon}\|\alpha\|_\infty \leq \bar{\epsilon}, \\
&\iff \|\sigma\|_\infty - \bar{\epsilon}\|\alpha\|_\infty \leq \bar{\epsilon}, \\
&\iff \|\sigma\|_\infty \leq \bar{\epsilon}(1 + \|\alpha\|_\infty), \\
&\implies \|\sigma\|_\infty \leq \bar{\epsilon}(1 + \|\alpha\|_1), \\
&\iff \|\sigma_k\|_\infty \leq \bar{\epsilon}(1 + \|\alpha\|_1), \quad \forall k \in \mathbb{Z}_{[0,p-1]},
\end{aligned}$$

where $\|D\sigma\|_\infty - \bar{\epsilon}\|\alpha\|_\infty \leq \|D\sigma - \bar{\epsilon}\alpha\|_\infty$ by reverse triangle inequality, $\|D\sigma\|_\infty = \|\sigma\|_\infty$ as multiplication by D appends zeros to σ, and $\|\alpha\|_\infty \leq \|\alpha\|_1$ for any vector α. This completes the proof. ☐

Remark 1. *While there are methods to linearize the constraint on $\|\sigma_k\|$ in (2d), the inclusion of $\|\alpha\|_1$ complicates the linearization of the constraint significantly. Furthermore, tightening the constraint to obtain $\|\sigma\|_\infty \leq \bar{\epsilon}(1+\|\alpha\|_\infty)$ is no longer compatible with linearization techniques on the infinity-norm as there are two separate infinity-norms in the inequality. To remedy this, Theorem 2 obtains a sufficient constraint involving just a single infinity-norm, to which the linearization can be readily applied to produce two linear inequalities. For more details on converting the infinity-norm to linear constraints in this manner, we refer the reader to reference [16]. From here, we may replace (2d) with the derived result $-D\sigma + \bar{\varepsilon}\alpha \leq t$ and $D\sigma - \bar{\varepsilon}\alpha \leq t$, which is indeed a set of linear constraints. While this constraint is indeed tighter than (2d), its compatibility with standard QP solvers preempts any need for generic, and more computationally-demanding, nonlinear solvers.*

V. Results and Discussion

For our constraint settings, we set $i_{\min} = -12$ A, $i_{\max} = -0.125$ A, $s_{\min} = 0$, $s_{\max} = 1$, $V_{p,\min} = -\infty$, $V_{p,\max} = +\infty$, $T_{c,\min} = 0$°C, $T_{c,\max} = 35$°C, and $T_a = 15$°C. We set the weights $\lambda_\alpha = 10^2$, $\lambda_\sigma = 10^3$, $q_{\text{tr}} = 1$, $q_i = q_V = 10^{-1}$, and $q_s = \beta q_{\text{tr}}$, where we assign various values to β to observe the impact of prioritizing charging speed compared to temperature rise. We inject uniformly distributed noises

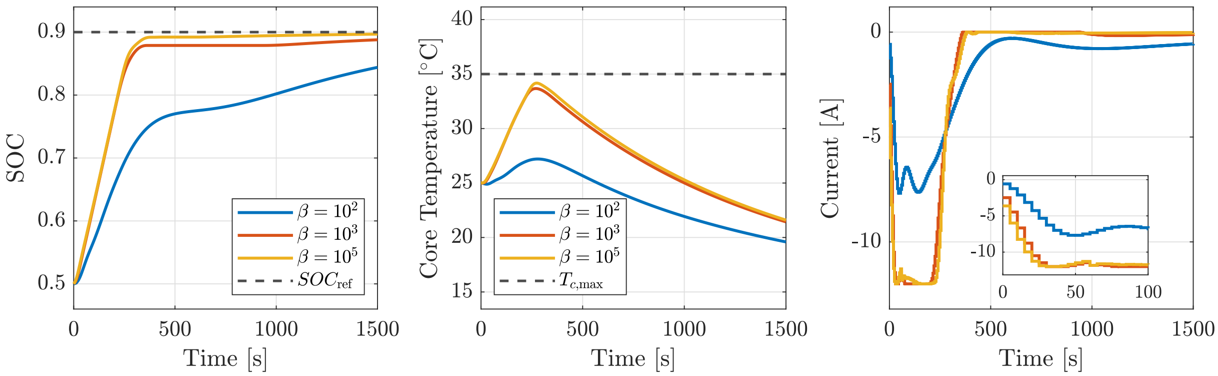

Fig. 1. DeePC charging performance under various values of β, with SOC (left), core temperature (middle), and current (right). Note that the larger β is, the more emphasis is placed on SOC tracking error.

$\bar{\varepsilon}_{SOC} = 0.01$ and $\bar{\varepsilon}_{T_c} = 0.5$ into the Hankel matrices, so $\bar{\varepsilon} = \max\{\bar{\varepsilon}_{SOC}, \bar{\varepsilon}_{T_c}\}$. To ensure optimal predictive control, we take disjoint segments of pseudorandom binary sequences collected over 5000 seconds with initial condition horizon $n = 10$ ($\alpha \in \mathbb{R}^{992}$) as the persistently-exciting signal, producing a control Hankel matrix of full row rank per Theorem 1. The corresponding QP was formulated for (2) and implemented in MATLAB 2024b on an Intel Core Ultra 7 running at 2100 MHz. The system used for experimentation is a Simulink-in-the-loop electrothermal battery model provided by the authors in [17], and the results are shown in Fig. 1 for a simulated time of 1500 seconds in 5-second increments.

As demonstrated by Fig. 1, the choice of the regularization weight β has a pronounced effect on the trade-off between SOC tracking performance and thermal safety. Control strategies that employ larger values of β converge to the reference $SOC_{\text{ref}} = 0.9$ significantly more quickly; for instance, the case $\beta = 10^5$ reaches within 1% of the target SOC after approximately 500 seconds, indicating rapid and aggressive charging. In contrast, strategies with more conservative regularization exhibit markedly slower convergence; the case $\beta = 10^2$ remains within only $\approx 6\%$ of the target SOC by the time the simulation period concludes, reflecting a deliberate prioritization of thermal and degradation constraints over tracking speed. Meanwhile, this improvement in convergence rate comes at the expense of generally larger core temperatures. More specifically, conservative values of β maintain core temperatures comfortably below 30°C throughout the simulation and produce comparatively mild current profiles, with $\|i_{(\beta=10^2)}\|_\infty \approx 7.5$A. By contrast, more aggressive charging strategies associated with large β drive the cell temperature higher beyond 30°C, nearly reaching the upper safety limit of 35°C. This observation underscores the inherent conflict between fast-charging objectives and the thermal management requirements that are critical for preserving long-term cell health and mitigating cell degradation. We also remark that the conservative strategy $\beta = 10^2$ yields a steady-state charging rate of approximately 0.816C, which falls favorably within the widely accepted safety window of 0.5C-1C that is commonly recommended in the literature to mitigate the risk of early-life lithium plating [18], [19].

To observe how the DeePC-generated optimal charging strategy behaves under a variety of thermal constraints, Fig. 2 considers $\beta = 10^5$ under three different core temperature constraints: 37°C, 38°C, and 39°C, with $\lambda_\alpha = 10^4$ to discourage trajectories that overfit to the initial conditions. The results indicate consistent observance of the temperature constraints across all three cases. Compared to the unconstrained results of Fig. 1 for $\beta = 10^5$, where SOC converges closely to the reference within 500 seconds, all thermally constrained SOC trajectories converge noticeably slower – particularly the case $T_{c,max} = 37$°C, which requires approximately 1500 seconds to reach SOC = 0.9 as the control sequences grow more conservative to avoid violating the thermal constraint. Of particular note is the behavior of the $T_{c,max} = 37$°C trajectory. For roughly the first 250 seconds, its SOC values overlap almost completely with the profiles for the more relaxed thermal constraints. However, at that point the core temperature approaches the constraint boundary, and the SOC profile deviates from the others, adopting a gradually-increasing, near-linear curve. This conservative charging behavior has the effect of keeping the core temperature near the boundary, demonstrating the controller's tendency to charge as quickly as possible without overshooting the thermal constraint. We also note that the current oscillates heavily during this period, effectively "balancing" the core temperature on the boundary without violation. Only after the SOC settles within a small neighborhood of the reference does the current go to zero and the core temperature decrease towards the ambient temperature of 35°C.

VI. Conclusion

As shown above, the application of data-enabled predictive control (DeePC) to electric vehicle optimal charging problem highlights promising ability to strike a balance between SOC reference tracking and mitigation of temperature rise. The investigated robust DeePC approach relaxes the accuracy requirement on measurement tool in the form of bounded additive noise $\epsilon_k \leq \bar{\epsilon}$, while the adaptation of the previously-nonlinear robust constraint into a sufficient linear constraint

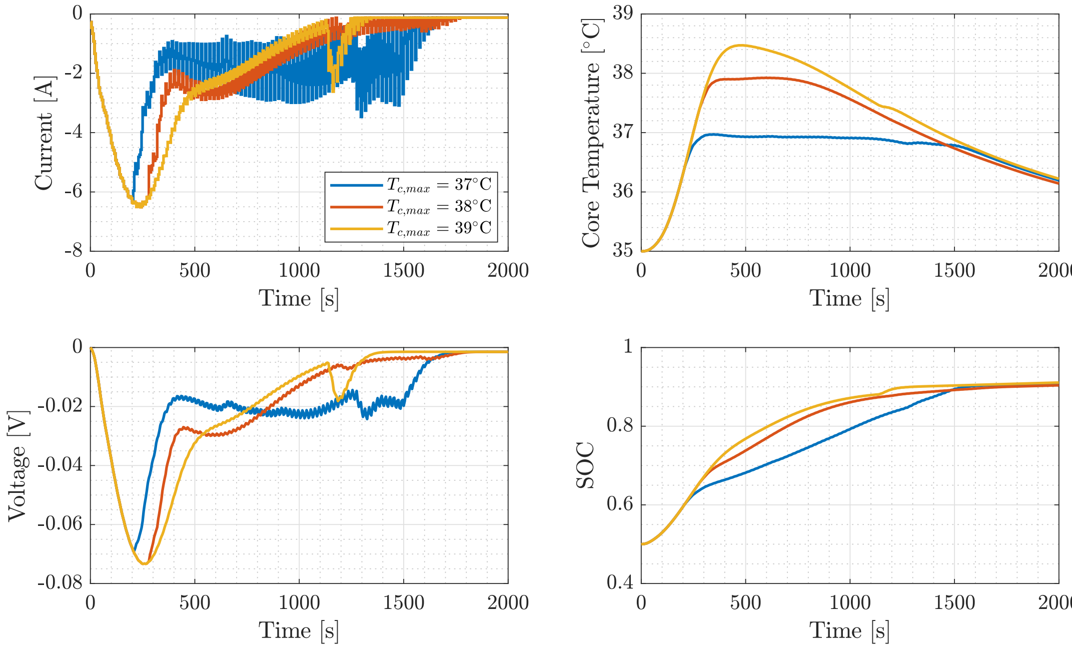

Fig. 2. DeePC charging performance at $T_{amb} = 35°C$ under three different constraints on core temperature, with current (top left), core temperature (top right), relaxation voltage (bottom left), and SOC (bottom right).

shows promise as a computationally-efficient and viable alternative, removing the need to accommodate resource-intensive nonlinear solvers in online control scenarios. Future work includes, but is not limited to:

1) Further adaptation of system constraints consistent with battery management systems to mitigate early-life plating and accelerated degradation.
2) Investigating adaptive Hankel matrix replacement for battery parameter changes at MoL (middle-of-life) and EoL (end-of-life), and further validation on hardware.
3) Rigorously establishing the tightness of the proposed linear constraint, and considering alternative bounds that preserve linearity yet are more loose, mitigating the risk of infeasibility for the corresponding QP problem.

REFERENCES

[1] S. Adams and A. O. Acheampong, "Reducing carbon emissions: the role of renewable energy and democracy," *Journal of Cleaner Production*, vol. 240, p. 118245, 2019.

[2] W. Yang, M. R. Hajidavalloo, Z. Li, and J. Chen, "Nmpc-based cell-level thermal management of ev batteries in low temperature environment," in *Modeling, Estimation and Control Conference*, Pittsburgh, PA, USA, October 5–8 2025. [Online]. Available: https://jchen2020.net/pubs/c_mecc2025-n.pdf

[3] D. Deng, "Li-ion batteries: basics, progress, and challenges," *Energy Science & Engineering*, vol. 3, no. 5, pp. 385–418, 2015.

[4] L. Song, Y. Zheng, Z. Xiao, C. Wang, and T. Long, "Review on thermal runaway of lithium-ion batteries for electric vehicles," *Journal of Electronic Materials*, vol. 51, no. 1, pp. 30–46, 2022.

[5] Y. Li, K. Li, Y. Xie, J. Liu, C. Fu, and B. Liu, "Optimized charging of lithium-ion battery for electric vehicles: Adaptive multistage constant current–constant voltage charging strategy," *Renewable Energy*, vol. 146, pp. 2688–2699, 2020.

[6] J. Li, E. Murphy, J. Winnick, and P. A. Kohl, "The effects of pulse charging on cycling characteristics of commercial lithium-ion batteries," *Journal of Power Sources*, vol. 102, no. 1–2, pp. 302–309, 2001.

[7] S. Pramanik and S. Anwar, "Electrochemical model based charge optimization for lithium-ion batteries," *Journal of Power Sources*, vol. 313, pp. 164–177, 2016.

[8] X. Hu, S. Li, and H. Peng, "A comparative study of equivalent circuit models for li-ion batteries," *Journal of Power Sources*, vol. 198, pp. 359–367, 2012.

[9] M. Schwenzer, M. Ay, T. Bergs, and D. Abel, "Review on model predictive control: An engineering perspective," *The International Journal of Advanced Manufacturing Technology*, vol. 117, no. 5, pp. 1327–1349, 2021.

[10] K. S. Holkar and L. M. Waghmare, "An overview of model predictive control," *International Journal of Control and Automation*, vol. 3, no. 4, pp. 47–63, 2010.

[11] J. C. Willems, P. Rapisarda, I. Markovsky, and B. L. M. De Moor, "A note on persistency of excitation," *Systems & Control Letters*, vol. 54, no. 4, pp. 325–329, 2005.

[12] J. C. Willems, "The behavioral approach to open and interconnected systems," *IEEE Control Systems Magazine*, vol. 27, no. 6, pp. 46–99, 2007.

[13] J. Coulson, J. Lygeros, and F. Dörfler, "Data-enabled predictive control: In the shallows of the deepc," in *Proceedings of the 18th European Control Conference (ECC)*, 2019, pp. 307–312.

[14] J. Berberich, J. Köhler, M. A. Müller, and F. Allgöwer, "Data-driven model predictive control with stability and robustness guarantees," *IEEE Transactions on Automatic Control*, vol. 66, no. 4, pp. 1702–1717, 2020.

[15] J. C. Willems, P. Rapisarda, I. Markovsky, and B. L. M. De Moor, "A note on persistency of excitation," in *Systems & Control Letters*, vol. 54, no. 4, 2005, pp. 325–329.

[16] A. Bemporad, F. Borrelli, and M. Morari, "Model predictive control based on linear programming: the explicit solution," *IEEE Transactions on Automatic Control*, vol. 47, no. 12, pp. 1974–1985, 2002.

[17] H. E. Perez, J. B. Siegel, X. Lin, A. G. Stefanopoulou, Y. Ding, and M. P. Castanier, "Parameterization and validation of an integrated electro-thermal cylindrical lfp battery model," in *Dynamic Systems and Control Conference*, vol. 45318, 2012, pp. 41–50.

[18] M. Petzl, M. Kasper, and M. A. Danzer, "Lithium plating in a commercial lithium-ion battery – a low-temperature aging study," *Journal of Power Sources*, vol. 275, pp. 799–807, 2015. [Online]. Available: https://www.sciencedirect.com/science/article/pii/S0378775314018928

[19] Z. Gao, H. Xie, X. Yang, W. Niu, S. Li, and S. Chen, "The dilemma of c-rate and cycle life for lithium-ion batteries under low temperature fast charging," *Batteries*, vol. 8, no. 11, p. 234, 2022.